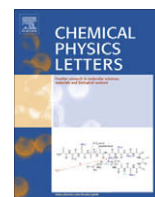




Contents lists available at ScienceDirect

Chemical Physics Letters

journal homepage: www.elsevier.com/locate/cplett

Efficient self-consistent DFT calculation of nondynamic correlation based on the B05 method

Emil Proynov, Yihan Shao, Jing Kong*

Q-Chem Inc., 5001 Baum Boulevard, Suite 690, Pittsburgh, PA 15213, USA

ARTICLE INFO

Article history:

Received 26 March 2010

In final form 10 May 2010

Available online 13 May 2010

ABSTRACT

Becke's B05 method of describing nondynamic electron correlation in Density Functional Theory is implemented self-consistently with computational efficiency. Important modifications of the method are proposed in order to make the self-consistency feasible. Resolution-of-identity technique is used to reduce dramatically the cost of the required exact-exchange energy density. The method is briefly validated on a variety of properties. It describes accurately for the first time the subtle energetics of the NO dimer, an exemplary system of strong nondynamic correlation. The efficient algorithm for the exact-exchange energy density can be applied to other functionals that use this quantity.

© 2010 Elsevier B.V. All rights reserved.

1. Introduction

Describing systems with strong nondynamic electron correlation is a major challenge of Density Functional Theory (DFT) [1–3]. Systems with strong nondynamic correlation include dissociating molecules, transition states of reactions, transition-metal compounds, strongly correlated solids, and many others. Such systems are usually treated with multi-reference wavefunction based methods since the accuracy of common local and semi-local exchange–correlation (XC) functionals is unsatisfactory in such cases. Attempts to generalize the Kohn–Sham (KS) DFT scheme to handle multi-determinant states have met mixed success [3,4]. Alternatively, it has been argued that nondynamic correlation should in principle be feasible within the single-determinant KS approach [1,2]: the KS determinant is used just to yield the electron density, while all correlation effects should be taken care of by the XC functional. A significant breakthrough along this line was made by Becke with his post Hartree–Fock (HF) real-space correlation model B05 [1,5]. A different model of nondynamic correlation was suggested later on by Perdew and coworkers based on a thorough real-space analysis of the XC hole [2]. Other fundamentally different views on the matter have been recently advanced [6,7].

B05 has four linear parameters trained on thermo-chemistry data, and two non-linear parameters in the dynamic correlation term. The results reported in the literature are extremely promising. This has motivated us to develop a self-consistent-field (SCF) version of the method so that it can be of a general use. Such a task requires solving some serious obstacles within the original B05 formulation: (i) lack of an analytic expression for the B05 exchange hole; (ii) discontinuities of the B05 potential; (iii) prohibitive com-

putational cost. The only SCF results with B05 reported so far are due to the recent work of Arbuznikov and Kaupp [8]. However, they did not attempt to remove the discontinuities, nor did they present a practical SCF solution for open-shell systems. Moreover the calculations remain prohibitively expensive in practice.

2. Theoretical and computational details

The B05 method is a conceptually new idea based on a careful analysis of the exact exchange hole. This hole becomes artificially too delocalized along a chemical bond that is too stretched. Becke argued that the exact exchange hole of a given spin should then be deepened by the exchange hole of opposite spin [1]. In most cases this is the main component of the nondynamic correlation energy, given in B05 by:

$$E_C^{\text{nd-op}} = \frac{1}{2} \int f(\mathbf{r}) [\rho_\alpha(\mathbf{r}) U_{X\beta}^{\text{exact}}(\mathbf{r}) + \rho_\beta(\mathbf{r}) U_{X\alpha}^{\text{exact}}(\mathbf{r})] d\mathbf{r}, \quad (1)$$

where ρ_σ and $U_{X\sigma}^{\text{exact}}$ are the spin-resolved electron density and Slater exact exchange potential, respectively ($\sigma = \alpha, \beta$) [1,5]. The 'correlation factor' $f(\mathbf{r})$ measures the strength of nondynamic correlation at each point:

$$f = \min(f_\alpha, f_\beta, 1), \quad (2)$$

with

$$f_\alpha(\mathbf{r}) = \frac{1 - N_{X\alpha}^{\text{eff}}(\mathbf{r})}{N_{X\beta}^{\text{eff}}(\mathbf{r})}, \quad f_\beta(\mathbf{r}) = \frac{1 - N_{X\beta}^{\text{eff}}(\mathbf{r})}{N_{X\alpha}^{\text{eff}}(\mathbf{r})}. \quad (3)$$

In the above, $N_{X\sigma}^{\text{eff}}$ is a partial ('relaxed') hole normalization within a region of roughly atomic size. The actual estimate of $N_{X\sigma}^{\text{eff}}$ is done using the Becke–Roussel (BR) exchange model [9] as an auxiliary tool. The original BR exchange hole [9] reproduces the

* Corresponding author.

E-mail address: jkong@q-chem.com (J. Kong).

curvature of the exact exchange hole and is normalized to one. In B05 this normalization is relaxed, so that the Slater exchange potential from the BR model be equal to the exact $U_{X\sigma}^{\text{exact}}$ at each point. This leads to a non-linear equation for certain dimensionless function $x_{\sigma}(y)$ employed in B05:

$$\frac{(x_{\sigma} - 2)}{x_{\sigma}^2} \left(e^{x_{\sigma}} - 1 - \frac{x_{\sigma}}{2} \right) = y_{\sigma} \equiv -\frac{3}{4\pi} \frac{Q_{\sigma}}{\rho_{\sigma}^2} U_{X\sigma}^{\text{exact}}, \quad (4)$$

where $(-Q_{\sigma})$ is the curvature of the exact exchange hole [1]. The relaxed normalization of the auxiliary BR exchange hole can then be obtained as:

$$N_{X\sigma}^{\text{eff}} = \left(\frac{2}{3} \right)^{3/2} \pi \rho_{\sigma}^{5/2} e^{x_{\sigma}} \left[\frac{(x_{\sigma} - 2)}{x_{\sigma} Q_{\sigma}} \right]^{3/2}. \quad (5)$$

Instead of solving Eq. (4) numerically at each point as in the original B05 approach, we solve it analytically using an accurate non-linear interpolation of $x(y)$. Analytical fit of the B05 function $x(y)$ has been proposed in Ref. [10]. We follow a similar approach, using a somewhat different technique that provides better accuracy [11]. The values of $x(y)$ were first obtained numerically on a grid along the y axis. Then the y domain was divided in three regions: region I $(-\infty \leq y \leq 0.15)$, region II $(-0.1 \leq y \leq 1001)$, and region III $(1000 \leq y \leq +\infty)$. For region I, we have obtained the following accurate analytical representation of $x(y)$:

$$x(y) = g(y) \frac{P_1(y)}{P_2(y)}, \quad g(y) = 2 \frac{(2 \arctan(a_1 y + a_2) + \pi)}{2 \arctan(a_2) + \pi}, \quad (6)$$

$$P_1(y) = \sum_{i=0}^5 c_i y^i; \quad P_2(y) = \sum_{i=0}^5 b_i y^i, \quad (7)$$

where a_i, b_i, c_i are numerical coefficients given in the Appendix A. This form of $x(y)$ has a mean absolute error (MAE) of 6.38×10^{-6} , and mean absolute percentage error (MAPE) of 0.00051%. We have obtained an accurate fit of $x(y)$ in region II as well, using Thiele interpolation technique of continuous fractions [11] (see Appendix A):

$$x(y) = \frac{R_1(y)}{4R_2(y)}, \quad R_1(y) = \sum_{i=0}^6 d_i y^i, \quad R_2(y) = \sum_{i=0}^6 e_i y^i. \quad (8)$$

This form provides a MAE = 3.67×10^{-6} and MAPE = 0.000067%. In region III $x(y)$ is a slow varying function. We use there the interpolation form proposed by Arbuznikov and Kaupp (Eq. (30) of Ref. [10]), which is suitable for this region as well. We have slightly readjusted their parameter ε in order to conform better to the somewhat different partitioning of the y domain we use:

$$x(y) = \ln(y) \left[\frac{1 + \frac{1}{\ln(y)}}{\ln(y)} + \frac{1.23767}{\ln(y)} + \frac{9.37587}{\ln(y)^2} - \frac{19.4777}{\ln(y)^3} + \frac{13.6816}{\ln(y)^4} - 0.078655 \right]. \quad (9)$$

The attained accuracy in this region (MAE = 0.0032) is about the same as the one reported in Ref. [10].

Besides the opposite-spin component, the same-spin contribution to the nondynamic correlation was modeled by Becke at a later stage [5]. It is a second-order correction to the exact exchange hole in open-shell systems:

$$E_C^{\text{nd-par}} = -\frac{1}{2} \int \left[\rho_{\alpha} A_{\alpha\alpha} M_{\alpha}^{(1)} + \rho_{\beta} A_{\beta\beta} M_{\beta}^{(1)} \right] d\mathbf{r}, \quad (10)$$

where $A_{\sigma\sigma}$ are second-order same-spin correlation factors, and $M_{\sigma}^{(1)}$ are the first-order moments of the BR auxiliary exchange hole (see Ref. [5] for details).

The final expression of the B05 energy functional reads:

$$E_{XC}^{\text{B05}} = E_X^{\text{HF}} + a_C^{\text{nd-opp}} E_C^{\text{nd-opp}} + a_C^{\text{nd-par}} E_C^{\text{nd-par}} + a_C^{\text{d-opp}} E_C^{\text{d-opp}} + a_C^{\text{d-par}} E_C^{\text{d-par}}, \quad (11)$$

where a_C^i are the four linear parameters in B05. The last two terms in Eq. (11) involve a dynamic correlation functional. Becke employed his meta-GGA correlation functional BR94 [12] which is quite accurate but has no fully analytic formulation. We have implemented previously the BR94 functional analytically [11] and use that form in Eq. (11).

To achieve SCF convergence, the f and $A_{\sigma\sigma}$ factors in Eqs. (1) and (10), and their derivatives, must be continuous. The original f factor has two sources of derivative discontinuity: the strict upper limit of 1, and the $\min(\)$ function used in its definition, Eq. (2) [8]. We smoothen first the upper limit of f with a quadratic smoothing function to the first-order when f is very close to 1:

$$f_{\sigma}(\mathbf{r}) \leftarrow 1 - \frac{1}{4\delta} (f_{\sigma}(\mathbf{r}) - 1 - \delta)^2, \quad |f_{\sigma}(\mathbf{r}) - 1| \leq \delta, \quad (12)$$

where parameter δ here is a small number to be specified. With this modification the correlation factor becomes: $f = \min(f_{\alpha}, f_{\beta})$. Strictly speaking, f is positively defined, since the relaxed hole normalization should not exceed 1. In practice $N_{X\sigma}^{\text{eff}}$ may occasionally exceed 1 (then f becomes negative). This excess is allowed in Becke's original model, while it is excluded in Ref. [8]. We have found that enforcing the condition $N_{X\sigma}^{\text{eff}} \leq 1$ leads to a deterioration of the B05 results in practice. Fully relaxing this condition however, leads to difficulties of the SCF procedure in a number of cases, a finding that we share with Ref. [8]. Our tests have shown that $N_{X\sigma}^{\text{eff}}$ may indeed exceed 1 for a number of points, but rarely goes larger than 2 if a high numerical accuracy is maintained. Thus, we introduce the condition $N_{X\sigma}^{\text{eff}} \leq 2$, and enforce it in a smooth manner, similar to Eq. (12). This greatly subdues the side effects of having negative f at some points, while preserves to a large extent the original B05 estimates.

Next, we smoothen the effect of the $\min(\)$ function in f using a Heaviside function:

$$H(z) = \frac{e^{pz}}{1 + e^{pz}}, \quad z = f_{\alpha} - f_{\beta}, \quad (13)$$

$$f = f_{\alpha} - zH(z). \quad (14)$$

This brings a second smoothening parameter p that controls how sharp the Heaviside function $H(z)$ is. Heaviside function is also used for the smoothening of the second-order factors $A_{\sigma\sigma}$, which involves a third parameter (q). The values of these smoothening parameters used here are: $\delta = 0.005$; $p = 115.0$; $q = 120.0$. Small variations around these values do not change noticeably the energies. Their fine tuning was done with respect to accelerating the SCF patterns as much as possible.

Having the relaxed BR exchange hole in an analytic form and the f and $A_{\sigma\sigma}$ factors smoothened, enable a feasible B05 SCF algorithm. Still, the computational cost of it is very high in the original implementation, since the exact-exchange energy density used in Eq. (4) is required at each grid point:

$$\rho_{\sigma} U_{\sigma}^{\text{exact}} \equiv V_{X\sigma}^{\text{exact}}(\mathbf{r}) = -\sum_{\mu\nu\lambda\omega} P_{\mu\nu}^{\sigma} P_{\lambda\omega}^{\sigma} \phi_{\mu}(\mathbf{r}) \phi_{\nu}(\mathbf{r}) \int \frac{1}{|\mathbf{r} - \mathbf{r}'|} (\phi_{\lambda}(\mathbf{r}') \phi_{\omega}(\mathbf{r}')) d\mathbf{r}', \quad (15)$$

where ϕ s are atomic basis functions, $P_{\mu\nu}$ are density matrix elements. As one can see, the calculation of $V_{X\sigma}^{\text{exact}}$ at each grid point using Eq. (15) requires looping over four atomic indexes. This has a computational cost similar to that of calculating the total HF energy analytically. There are thousands of grid points for each atom, making it prohibitively expensive. In this work we explore a cost-

effective alternative of calculating V_X^{HF} based on a specific use of the resolution-of-identity (RI) approximation [13]. We first expand a given basis-function pair (BFP) $\phi_\mu\phi_\nu$ as a linear combination of auxiliary basis functions X_m of Gaussian type with $C_m^{\mu\nu}$ being the RI fitting coefficients.

$$\phi_\mu(\mathbf{r})\phi_\nu(\mathbf{r}) \approx \sum_m C_m^{\mu\nu} X_m(\mathbf{r}), \quad (16)$$

Using this expansion in the density of molecular-orbital (MO) pairs ρ_{ij} gives:

$$\rho_{ij}^\sigma(\mathbf{r}) = \sum_{\mu\nu m} C_{i\mu}^\sigma C_{j\nu}^\sigma C_m^{\mu\nu} X_m(\mathbf{r}) = \sum_m C_m^{ij,\sigma} X_m(\mathbf{r}), \quad (17)$$

where $C_{i\mu}^\sigma$ are the MO coefficients of the occupied MOs. This leads to (the spin index σ is omitted for abbreviation):

$$\begin{aligned} V_X^{\text{exact}} &= - \sum_{mn} X_m(\mathbf{r}) \int \frac{1}{|\mathbf{r}-\mathbf{r}'|} X_n(\mathbf{r}') d\mathbf{r}' \sum_{ij}^{\text{occ}} C_m^{ij} C_n^{ij} \\ &\equiv - \sum_{mn} V_{mn}(\mathbf{r}) B_{mn}. \end{aligned} \quad (18)$$

In contrast to Eq. (15), the calculation of the approximate $V_{mn}(\mathbf{r})$ with Eq. (18) involves only two atomic function indices, effectively reducing the scaling of calculation by two orders.¹ The evaluation of B_{mn} is a linear-algebra operation that does not depend of the numerical grid.

Finally the B05 SCF potential is obtained after taking the derivatives of the new energy components (Eq. (1) + Eq. (10)) with respect to \mathbf{P} , following the standard methodology, ca. Ref. [14]:

$$F_{\mu\nu}^{\text{nd},\sigma} = \frac{\partial(E_C^{\text{nd-op}} + E_C^{\text{nd-par}})}{\partial P_{\mu\nu}^\sigma}. \quad (19)$$

The resulting expressions are quite complicated and lengthy and will be presented elsewhere. It suffices to say that $E_C^{\text{nd-op}}$ and $E_C^{\text{nd-par}}$ are now fully differentiable due to the improved analytical interpolation of relaxed BR exchange-hole function and the removal of the discontinuities in the original B05 model. Furthermore, the computational efficiency is dramatically improved.

The above algorithm is implemented in a development version of Q-CHEM Program [15]. All calculations are carried out using G3LARGE basis set [16] and an unpruned grid composed of 128 radial points and 194 angular points per atomic region. Converged LDA electron density is used as initial guess, which greatly improves the B05 SCF convergence. An accurate RI calculation of the exact-exchange energy density requires auxiliary bases larger than in most other RI applications. We have created a new RI basis library by enlarging an existing RI basis [13] in an even-tempered manner. With the new auxiliary basis the RI error in reproducing the exact-exchange energy is typically about 10^{-7} – 10^{-5} a.u. We have compared our RI-B05 results with the original published B05 values [17] of the exact exchange energies and the nondynamic correlation energies of atoms (see Supplementary Table 1, Appendix B). The mean-absolute-deviation between the two sets of values is 0.001 a.u. for both properties, which absorbs also the effects of the different basis set and grid used in Ref. [17].

3. Results and discussions

RI provides a great gain in efficiency. For instance, the calculation of the B05 energies of pyrrole and benzene, with a direct implementation of Eq. (15), takes 447 and 1154 min per iteration, respectively, on an AMD Opteron processor, and only 8 and 12 min, respectively, with RI (Supplementary Table 2, Appendix B). This

technique should be useful also for other functionals employing V_X^{exact} , the so-called fourth rung functionals [2]. A different algorithm for the exact-exchange energy density has been proposed by Gorling et al. [18]. It uses the basis functions themselves in the RI expansion, resulting in a convenient formulism that requires only the standard HF exchange matrix. However, subsequent applications have shown that this method demands large, uncontracted basis sets [2], which is rather inconvenient for routine calculations. Our algorithm on the other hand applies to any orbital basis set from the standard basis set libraries.

A preliminary assessment of RI-B05, with and without SCF, is done through benchmark calculations of atomization energies, bond lengths and reaction barriers (Appendix B). The atomization energies are calculated on the Lap test set of rapid XC assessment [14,19] (Supplementary Table 3 (Appendix B)). This set has been used on various occasions before. It provides a sample statistics for functional assessment that is qualitatively similar to that based on larger data sets like G2 or G3, while saves a significant amount of time. Becke's original post-LDA B05 implementation yields very accurate atomization energies [5]. When used in post-LDA manner, our RI-B05 gives MAE of 2.18 kcal/mol on the Lap test set. For comparison, M06, B3LYP, and B3tLAP hybrid schemes [20] give MAE of 2.63, 2.17, and 2.08 kcal/mol, respectively, on the same set. The SCF-RI-B05 atomization energies deviate somewhat more (MAE of 3.3 kcal/mol). The values are in most cases somewhat smaller than the original B05 estimates, which shows a possibility of improvement by re-optimizing the original B05 parameters self-consistently.

The SCF implementation of RI-B05 allows to assess its accuracy on optimized geometries. We have calculated the bond lengths of a series of diatomic molecules from the Lap test set [14]. Previous studies have shown [14,20] that the B3LYP functional continues to yield one of the best geometries for small and medium size molecules. It is rather encouraging that the SCF-RI-B05 optimized bond lengths (MAE 0.0045 Å) are slightly more accurate than those of B3LYP (MAE 0.0053 Å) on the present test set (Supplementary Table 4, Appendix B). The implementation of the analytic gradient of RI-B05 is in progress.

An accurate prediction of reaction barriers requires an adequate description of nondynamic correlation. It is where the benchmarks by Dickson and Becke [21] have shown the major strength of B05. Table 1 contains the calculated classical barriers for 18 'difficult' reactions comparing several methods: RI-B05, SCF-RI-B05, M06-2X, B3tLap, B3LYP.

The first two columns of Table 1 compare our post-LDA RI-B05 results with the original post-LDA B05 data of Dickson and Becke [23]. The agreement between the two is very good. The observed small deviations between the two sets of data are mainly due to the different basis sets and grids used. The post-LDA RI-B05 results have the smallest MAE (1.3 kcal/mol) here, better than the M06-2X functional [22] (MAE of 1.5 kcal/mol) optimized particularly for reaction barriers. The accuracy of B3LYP on these reactions is poor (MAE of 5.5 kcal/mol). The recent hybrid functional B3tLap [20] shows some improvement over B3LYP here (MAE of 2.9 kcal/mol) but remains behind B05. The SCF-RI-B05 version slightly underestimates the energy barriers in most cases, compared the original B05 values, which leads to a slight increase of MAE (1.7 kcal/mol). This shows again the necessity of re-optimizing the original B05 parameters in the SCF context.

Having presented a brief assessment of RI-B05, we turn to one uncharted application of this method, the subtle case of *cis* NO dimer (ONNO). This is an exemplary system of strong nondynamic correlation that is rather difficult to describe. The usual Lewis picture of each monomer sharing a single electron to form a covalent N–N bond pair is not adequate here. Instead, the experiment indicates a very weak binding energy (D_e) of the order of

¹ The V matrix needs to be symmetrized before using it.

Table 1
The classical barriers for 18 'most difficult' reactions (f = forward, r = reverse).

Reaction		B05/B ^a	RI-B05 ^b	RI-B05-SCF	M06-2X	B3tLap	B3LYP	Ref. ^c
H + HCl ↔ H ₂ + Cl	f	6.0	5.8	4.1	4.3	3.8	0.7	5.7
	r	9.0	9.2	7.0	6.8	6.3	4.4	8.7
H + HCl ↔ HCl + H		17.4	17.7	17.0	18.1	16.3	12.7	18.0
H + OH ↔ H ₂ + O	f	8.3	7.8	6.7	9.2	7.3	4.0	10.7
	r	12.7	12.8	11.4	11.7	9.0	6.2	13.1
F + H ₂ ↔ HF + H	f	3.0	3.0	-1.7	1.0	-3.6	-5.6	1.8
	r	35.5	35.1	30.6	31.5	26.8	23.2	33.4
H + H ₂ ↔ H ₂ + H		10.3	10.4	8.8	11.6	7.5	4.3	9.6
OH + H ₂ ↔ H + H ₂ O	f	6.0	5.6	3.5	4.6	3.1	0.8	5.1
	r	21.5	21.3	19.0	20.8	17.4	13.3	21.2
OH + NH ₃ ↔ H ₂ O + NH ₂	f	3.6	3.2	2.4	2.2	-0.5	-2.3	3.2
	r	13.7	13.2	12.0	11.8	8.9	7.2	12.7
H + H ₂ S ↔ HS + H ₂	f	2.7	3.1	2.3	4.5	2.6	-0.4	3.5
	r	17.6	17.9	16.1	18.1	16.5	15.9	17.3
O + HCl ↔ OH + Cl			15.8	8.9	7.3	4.2	1.5	9.8
			14.2	7.1	7.1	5.0	4.4	10.4
H + CH ₃ OH ↔ H ₂ + CH ₂ OH	f	9.6	9.8	8.2	10.1	6.7	3.7	7.3
	r	16.0	15.7	13.7	15.8	14.1	13.2	13.8
MAE on 18 reactions			1.3	1.7	1.5	2.9	5.5	

^a Results from post-SCF-B05 of Ref. [21].

^b Post-SCF-RI-B05 results of the present work.

^c Best available reference values from the Truhlar's online data base (<http://comp.chem.umn.edu/database>).

Table 2
Singlet–triplet split Δ_{T-S} (kcal/mol), dimerization energy D_e (kcal/mol, BSSE corrected), and geometry (R_{N-N} and R_{N-O} in Å, $\angle NNO$ in degree) of *cis* NO dimer ONNO.

	HF	B3LYP	BP	B3tLap	M06-2X	SCF-B05	MRCI	Expt ^c
Δ_{T-S}	-49.2	-2.3	-4.9	+0.3	+4.0	+5.5	+6.3 ^b	
D_e	-49.6	-3.1	9.7	-0.9	-6.7	3.5	3.3 ^a	2.9–3.3
R_{N-N}	1.613	1.972	2.045	1.982	1.828	1.994	2.284 ^a	2.263
R_{N-O}	1.132	1.147	1.160	1.149	1.143	1.150	1.149 ^a	1.152
$\angle NNO$	110.1	101.5	99.9	102.4	104.4	101.5	96.1 ^a	97.17

^a Results of Ref. [24].

^b $\Delta_{T-S} = E(^3B_1) - E(^1A_1)$ from Ref. [25]. Positive Δ_{T-S} means the singlet is more stable.

^c Data from Refs. [28,29].

2.9–3.3 kcal/mol [23], the *cis* ONNO configuration being the most stable. It has been found by several multi-reference (MR) studies [24–27] that the NO dimer bonding has a strong multi-reference character, the most stable conformation being indeed the singlet *cis* form, with 1A_1 type ground state and $D_e \sim 3.3$ kcal/mol, in good agreement with the experiment. The closest triplet state, 3B_1 , is about 6.3 kcal/mol higher [25]. Wavefunction methods based on single HF reference such as MP2, and even CCSD(T), fail to predict the correct energy ordering here [23,27]. The early DFT studies reported in literature [23] give a triplet ground state, in contradiction to experiment. Table 2 summarizes our results for the singlet state dimerization energy and the singlet–triplet split of *cis* ONNO obtained with SCF-RI-B05 and several other methods, along with benchmarks from MRCI and experiment. The singlet–triplet split is calculated at the optimized geometries of both respective states. HF yields the wrong ground state (the triplet) which is off by a large margin (49 kcal/mol). B3LYP fails too in a similar way but with much smaller margin. The recent hybrid functionals, B3tLap and M06-2X give a qualitatively correct singlet–triplet ordering, but rather small split compared to the MRCI benchmark. The SCF-RI-B05 estimate is the closest to the MRCI benchmark here. Considering next the dimerization energy, the SCF-RI-B05 estimate is in excellent agreement with MRCI and experiment. HF and all the hybrid DFT methods predict an unbound dimer, with HF being off by the largest margin. The dimerization energy obtained with the pure-GGA method BP (Becke 88 exchange with Perdew 86 correlation) has the right sign, but is too large. The single-determinant methods (HF and DFT) yield shorter N–N distances and larger N–

N–O angles than the benchmark values. The SCF-RI-B05 scheme produces relatively better N–N bond length among the methods that yield singlet ground state, but still it is too short. We have calculated the ONNO energy also at its fixed experimental geometry. All the methods tested here yield slightly smaller D_e and Δ_{T-S} at the experimental ONNO geometry. The SCF-RI-B05 gives in this case $D_e = 2.77$ kcal/mol, $\Delta_{T-S} = 5.3$ kcal/mol, still in excellent agreement with the experiment.

The failure of HF for this strongly correlated system is no surprise, given the lack of electron correlation in this method and the large separation of the two NO monomers. This causes an artificially strong delocalization of the HF exchange hole. Unlike HF, the exchange–correlation hole underlying the popular pure-GGA functional BP is localized in space. This provides a significant improvement over HF, but still fails to give the right singlet–triplet ordering and over-binds the dimer. B05 compensates precisely the artificial delocalization of the HF exchange, after measuring it at each point in space, and yields the right energetics for this system. The subtle nondynamic correlation here cannot be properly described without explicitly including it in the underlined physical model.

4. Conclusions

Combining a 100% HF exchange with a proper correlation functional has been a long-standing problem in DFT. The recently developed B05 functional by Becke is a breakthrough along this

line. However, its original formulation is prohibitively expensive. In this work we represent the B05 functional in a fully analytic, continuous form that allows a consistent and efficient SCF implementation, with a considerable speed up. The preliminary validation results promising: SCF-RI-B05 yields excellent reaction barriers, especially concerning 'difficult' reactions, and very good bond lengths of diatomic molecules. It describes quite well (for the first time with DFT) the subtle energetics of the NO dimer, an exemplary system of strong nondynamic correlation. Further tests are ongoing to assess more fully this method, and to find ways of improving it further.

Acknowledgments

The work is supported by a Grant from National Institute of Health (GM081928). The authors wish to thank Dr. Zhengting Gan for technical assistance. The authors also thank Dr. Axel Becke for helpful discussions, and for the confirmation that he used the same upper limit of 2 on the effective normalization of the relaxed exchange hole in his implementation of B05.

Appendix A

The two interpolation coefficients in Eq. (6) read

$$a_1 = 0.9301841768238374, a_2 = 0.5485569431916153.$$

The values of the coefficients c_i and b_i entering Eq. (7) read:

$$\begin{aligned} c_0 &= -5.968528012907202; c_1 = -2.183747742603848; \\ c_2 &= -4.985886441243756; c_3 = -1.134161212063683; \\ c_4 &= -1.692142642619975; c_5 = 0.5708959538346894; \\ b_0 &= -5.968528013066088; b_1 = -2.030780232084790; \\ b_2 &= -4.679675048001286; b_3 = -1.118849057754117; \\ b_4 &= -1.808705503402923; b_5 = 0.5922648216175291. \end{aligned}$$

The values of the coefficients d_i and e_i entering Eq. (8) read:

$$\begin{aligned} d_0 &= 268.8413661379433; d_1 = 469.6693640414017; \\ d_2 &= 331.7800151829805; d_3 = 99.40088877152307; \\ d_4 &= 8.786661786414733; d_5 = 0.1643722176146135; \end{aligned}$$

$$\begin{aligned} d_6 &= 0.0003404244647727309. \\ e_0 &= 33.6051707672429; e_1 = 46.23703278485152; \\ e_2 &= 26.8894984040501; e_3 = 6.007166968496472; \\ e_4 &= 0.392204000640807; e_5 = 0.005438465669613952; \\ e_6 &= 0.0000078437439010087. \end{aligned}$$

Appendix B. Supplementary data

Supplementary data associated with this article can be found, in the online version, at doi:10.1016/j.cplett.2010.05.029.

References

- [1] A.D. Becke, *J. Chem. Phys.* 119 (2003) 2972.
- [2] J.P. Perdew, V.N. Staroverov, J. Tao, G.E. Scuseria, *Phys. Rev. A* 78 (2008) 052513.
- [3] M. Weimer, F. Della Sala, A. Gorling, *J. Chem. Phys.* 128 (2008) 144109.
- [4] J. Toulouse, P. Gori-Giorgi, A. Savin, *Theor. Chem. Acc.* 114 (2005) 305.
- [5] A.D. Becke, *J. Chem. Phys.* 122 (2005) 64101.
- [6] P. Gori-Giorgi, M. Seidl, G. Vignale, *Phys. Rev. Lett.* 103 (2009) 166402.
- [7] A.J. Cohen, P. Mori-Sanchez, W. Yang, *Science* 321 (2008) 792.
- [8] A.V. Arbuznikov, M. Kaupp, *J. Chem. Phys.* 131 (2009) 084103.
- [9] A.D. Becke, M.R. Roussel, *Phys. Rev. A* 39 (1989) 3761.
- [10] A.V. Arbuznikov, M. Kaupp, *J. Mol. Struct. (THEOCHEM)* 762 (2006) 151.
- [11] E. Proynov, Z. Gan, J. Kong, *Chem. Phys. Lett.* 455 (2008) 103.
- [12] A.D. Becke, *Int. J. Quant. Chem. Symp.* 28 (1994) 625.
- [13] Y.A. Jung, A. Stodt, P.M.W. Gill, M. Head-Gordon, *Proc. Natl. Acad. Sci. USA* 102 (2005) 6692.
- [14] E. Proynov, J. Kong, *J. Chem. Theory Comput.* 3 (2007) 746.
- [15] Y. Shao et al., *Phys. Chem. Chem. Phys.* 8 (2006) 3172.
- [16] L.A. Curtiss, K. Raghvachari, P.C. Redfern, V. Rassolov, J.A. Pople, *J. Chem. Phys.* 109 (1998) 7764.
- [17] A.D. Becke, E.R. Johnson, *J. Chem. Phys.* 127 (2007) 124108.
- [18] F. Della Sala, A. Gorling, *J. Chem. Phys.* 115 (2001) 5718.
- [19] E. Proynov, H. Chermette, D.R. Salahub, *J. Chem. Phys.* 113 (2000) 10013.
- [20] E. Proynov, J. Kong, in: G. Vayssilov, T. Mineva (Eds.), *Theoretical Aspects of Catalysis*, Heron Press, Sofia, 2008, p. 453.
- [21] R.M. Dickson, A.D. Becke, *J. Chem. Phys.* 123 (2005) 111101.
- [22] Y. Zhao, D.G. Truhlar, *J. Chem. Phys.* 125 (2006) 194101.
- [23] H.A. Duarte, E. Proynov, D.R. Salahub, *J. Chem. Phys.* 109 (1998) 26.
- [24] R. Gonzalez-Luque, M. Merchan, B.O. Ros, *Theor. Chim. Acta* 88 (1994) 425.
- [25] A.L.L. East, *J. Chem. Phys.* 109 (1998) 2185.
- [26] S.V. Levchenko, H. Reisler, A.I. Krylov, O. Gessner, A. Stolow, H. Shi, A.L.L. East, *Chem. Phys.* 125 (2006) 084301.
- [27] N. Taguchi, Y. Mochizuki, T. Ishikawa, K. Tanaka, *Chem. Phys. Lett.* 451 (2008) 31.
- [28] B.J. Howard, A.R.W. McKellar, *Mol. Phys.* 78 (1993) 55.
- [29] J.R. Hetzler, M.P. Casassa, D.S. King, *J. Chem. Phys.* 95 (1991) 8086.